The AAPS Journal, Vol. 16, No. 3, May 2014 (© 2014)
DOI: 10.1208/s12248-014-9595-6

Research Article

Targeted Delivery of Curcumin to Tumors *via* PEG-Derivatized FTS-Based Micellar System

Yichao Chen,[1] Xiaolan Zhang,[1] Jianqin Lu,[1] Yixian Huang,[1] Jiang Li,[1] and Song Li[1,2]

Received 23 December 2013; accepted 11 March 2014; published online 5 April 2014

Abstract. Curcumin and S-*trans*, *trans*-farnesylthiosalicylic acid (FTS) are two promising anticancer agents. In this study, we demonstrated that the two agents exerted significant synergy in antitumor activity in various types of cancer cells with combination indices ranging from 0.46 to 0.98 (a value of less than unity indicates synergism). We have further shown that synergistic-targeted co-delivery of the two agents can be achieved *via* formulating curcumin in polyethylene glycol (PEG)-derivatized FTS-based nanomicellar system. Curcumin formulated in PEG-FTS micelles had small size of around 20 nm. The nanomicellar curcumin demonstrated enhanced cytotoxicity towards several cancer cell lines *in vitro*. Intravenous application of curcumin-loaded micelle (20 mg kg^{-1} curcumin) led to a significantly more effective inhibition of tumor growth in a syngeneic mouse breast cancer model (4T1.2) than curcumin formulated in Cremophor/EL ($P<0.05$).

KEY WORDS: curcumin; dual–functional carrier; micelles; synergy; S-*trans*, *trans*-farnesylthiosalicylic acid.

INTRODUCTION

Curcumin, a hydrophobic polyphenol compound extracted from *Curcuma longa*, has a wide spectrum of pharmacological activities and holds promise in the management of various diseases, such as cancers, cardiovascular diseases, Alzheimer's disease, and diabetes (1–5). Particularly, curcumin has drawn interests as a therapeutic and chemopreventive agent for cancers *via* suppressing multiple signaling pathways such as MAPKs, PI3K/AKT, and NF-κB and inhibiting tumor cell proliferation, invasion, metastasis, and angiogenesis with no obvious side effect (6–10). Moreover, curcumin acts as a chemosensitizer that augments the cytotoxic effect of other chemotherapeutic drugs such as doxorubicin and cisplatin (11–13).

S-*trans*, *trans*-farnesylthiosalicylic acid (FTS) is a synthetic farnesylcysteine mimetic that acts as a potent and especially nontoxic Ras antagonist (14,15). Constitutively active Ras caused by mutation in the Ras family of proto-oncogenes is present in one third of human cancers, with the highest incidence of mutational activation of Ras being detected in pancreatic and colon cancers (16,17). Ras is also activated in cancer cells by other mechanisms (18,19). FTS has been shown to cause significant reduction of Ras levels, showing antitumor activity in a wide range of human cancers without observable side effects (17,20–22). FTS also can work in combination with other anticancer drugs, such as valproic acid and PKF115-584 (23,24).

Both curcumin and FTS have issues of poor water solubility and limited oral bioavailability despite their potentials as anticancer agents (25,26). We have recently shown that PEGylation of FTS led to significantly increased solubility of FTS in aqueous solution (27). A conjugate of one molecule of PEG5000 (PEG_{5K}) with two molecules of FTS *via* a labile ester linkage (PEG_{5K}-FTS_2 (L)) well retained the FTS biological activity (27). Interestingly, polyethylene glycol (PEG)-derivatized FTS self-assembled to form small-sized micelles that are effective in solubilizing other hydrophobic drugs such as paclitaxel (PTX) (27). In addition, PEG-FTS-based micelles demonstrated synergistic antitumor activity with co-delivered PTX *in vitro* and *in vivo* (27). In this study, we examined whether the combination of curcumin and FTS exerted a synergy in antitumor activity in various types of tumor cells. The potential of PEG-FTS-based micellar system in synergistic-targeted delivery of curcumin was also investigated.

METHODS

Materials

Curcumin (synthetic) was purchased from TCI American (OR, USA). Dimethyl sulfoxide (DMSO), 3-(4,5-dimethylthiazol-2-yl)-2,5-diphenyl tetrazolium bromide (MTT), trypsin-EDTA solution, Triton X-100, and Dulbecco's Modified Eagle's Medium (DMEM) were all purchased from Sigma-Aldrich (MO, USA). FTS was synthesized and purified following the published literature (15). Antibodies against p-Akt (S473) and Akt were purchased from Santa Cruz Biotechnology. HRP-

Electronic supplementary material The online version of this article (doi:10.1208/s12248-014-9595-6) contains supplementary material, which is available to authorized users.

[1] Center for Pharmacogenetics, Department of Pharmaceutical Sciences, School of Pharmacy, University of Pittsburgh, 639 Salk Hall, Pittsburgh, PA 15261, USA.
[2] To whom correspondence should be addressed. (e-mail: sol4@pitt.edu)

labeled goat antirabbit IgG was purchased from Amersham Biosciences (Piscataway, NJ, USA). Dulbecco's phosphate-buffered saline (DPBS) was purchased from Lonza (MD, USA). Fetal bovine serum (FBS) and penicillin–streptomycin solution were from Invitrogen (NY, USA).

Cell Culture

4T1.2 is a mouse breast cancer cell line, and Panc02-H7 (H7) is a mouse metastatic pancreatic cancer cell line. DU145 and PC3 are two human androgen-independent prostate cancer cell lines. A549 is a human lung cancer cell line, and MCF7 is a human breast cancer cell line. All these cell lines were cultured in DMEM medium containing 10% FBS and 1% penicillin–streptomycin at 37°C in a humidified environment with 5% CO_2.

Animals

Female BALB/c mice (4–6 weeks) were purchased from Charles River Laboratories. All animals were housed at controlled temperature and humidity according to AAALAC guidelines. All animal-related procedures were performed by fully following the protocol guidelines approved by the Animal Use and Care Administrative Advisory Committee of the University of Pittsburgh.

Synthesis of PEG_{5K}-FTS_2 Conjugate

PEG_{5K}-FTS_2(L) is a conjugate of one molecule of PEG5000 (PEG_{5K}) with two molecules of FTS *via* a labile ester linkage. PEG_{5K}-FTS_2(S) is similar to PEG_{5K}-FTS_2(L) in structure but has a relatively stable amide linkage between PEG and FTS (27). PEG_{5K}-FTS_2(L) and PEG_{5K}-FTS_2(S) conjugates were synthesized and chemically characterized as described previously (27). Briefly, for the synthesis of PEG_{5K}-FTS_2(L), MeO-PEG_{5k}-OH (1 equiv.), succinic anhydride (5 equiv.), and 4-(dimethylamino) pyridine (DMAP, 5 equiv.) were mixed in DCM to yield carboxyl-terminated PEG monomethyl ether (MeO-PEG_{5k}-COOH). Diethanolamine (3 equiv.) was then coupled to the carboxylic group of MeO-PEG_{5k}-COOH (1 equiv.) using *N*-hydroxysuccinimide (NHS 3.6 equiv.) and dicyclohexylcarbodiimide (DCC 3.6 equiv.). PEG monomethyl ether with two hydroxyl groups (MeO-PEG_{5k}-$(OH)_2$) was purified by precipitation with ice-cold diethyl ether and ethanol respectively. PEG_{5K}-FTS_2(L) conjugate was obtained by coupling MeO-PEG_{5k}-$(OH)_2$ (1 equiv.) to FTS (5 equiv.) *via* DCC (3 equiv.) and DMAP (0.3 equiv.) in chloroform. The mixed solution was filtered, and the final product was purified by precipitation in cold diethyl ether and ethanol respectively. PEG_{5K}-FTS_2(S) was similarly synthesized except that MeO-PEG_{5k}-OH was first reacted with di-Boc lysine followed by deprotection of Boc using TFA. MeO-PEG_{5k}-$(NH_2)_2$ was then reacted with FTS *via* DCC and DMAP, and the final product was similarly purified as described above. The structures of PEG_{5K}-FTS_2(L) and PEG_{5K}-FTS_2(S) were confirmed by NMR (Figure S1).

Preparation of Curcumin-Loaded Micelles

Curcumin (10 mM in chloroform) was mixed with PEG_{5K}-FTS_2(L) or PEG_{5K}-FTS_2(S) (10 mM in chloroform) at various carrier/drug molar ratios. The chloroform was removed by a stream of nitrogen to generate a thin film at the bottom of the glass tube, and the residual organic solvent was further removed under vacuum for 2 h. Subsequently, the thin film was hydrated and suspended in DPBS to form the curcumin-loaded micelles. The unincorporated curcumin was removed by filtration through a syringe filter (pore size, 0.22 μm). The drug-free micelles were similarly prepared as described above.

Characterization of Curcumin-Loaded Micelles

The average size and *polydispersity* index (PDI) of blank and curcumin-loaded micelles were measured by Zetasizer (Zetasizer Nano ZS instrument, Malvern, Worcestershire, UK) under room temperature.

The morphology of micelles was examined through transmission electron microscopy (TEM). Briefly, curcumin micelles were diluted with DPBS and placed on a copper grid covered with Formvar. Samples were stained with 1% uranyl acetate, and imaging was performed at room temperature using TEM (JEM-1011, JEOL, Japan).

The drug-loading capacity (DLC) and drug-loading efficiency (DLE) of curcumin micelles were determined by reverse phase HPLC (Alliance, 2695–2998 system). Briefly, curcumin-loaded micelles were prepared as described above and then filtered through a syringe filter (0.22 μm). Curcumin in the filtered and nonfiltered micelles was extracted with methanol and quantified by HPLC with a mobile phase consisting of methanol/0.3% acetic acid (80/20, *v*/*v*), a flow rate at 1 mL/min, and a UV detector. The DLC and DLE of curcumin micelles were calculated according to the following formula:

$$\mathrm{DLC}(\%) = [\text{weight of drug used}/(\text{weight of polymer} + \text{drug used})] \times 100\%$$

$$\mathrm{DLE}\ (\%) = (\text{weight of loaded drug}/\text{weight of input drug}) \times 100\ \%$$

The colloidal stability of curcumin micelles with various carrier/drug molar ratios was evaluated by following the changes in sizes of the particles at different times following sample preparation.

Cytotoxicity Assay

Cytotoxicity assay was performed on 4T1.2, MCF7, A549, H7, DU145, and PC3 cell lines. All cells were plated at a density of 1,000 cells per well in 96-well plates and incubated for 24 h in DMEM with 2.5% FBS and 1% streptomycin/penicillin. Then, cells were treated with various concentrations of free FTS, free curcumin, and the combination of both respectively for 96 h. Viability of cells was evaluated by MTT assay as described (28).

To test the cytotoxicity of curcumin-loaded PEG_{5K}-FTS_2(L) or PEG_{5K}-FTS_2(S) micelles, cells were treated with indicated concentrations of free curcumin, drug-free micelles, and curcumin-loaded PEG_{5K}-FTS_2(L) or PEG_{5K}-FTS_2(S) micelles respectively for 96 h. MTT assay was then performed as described above.

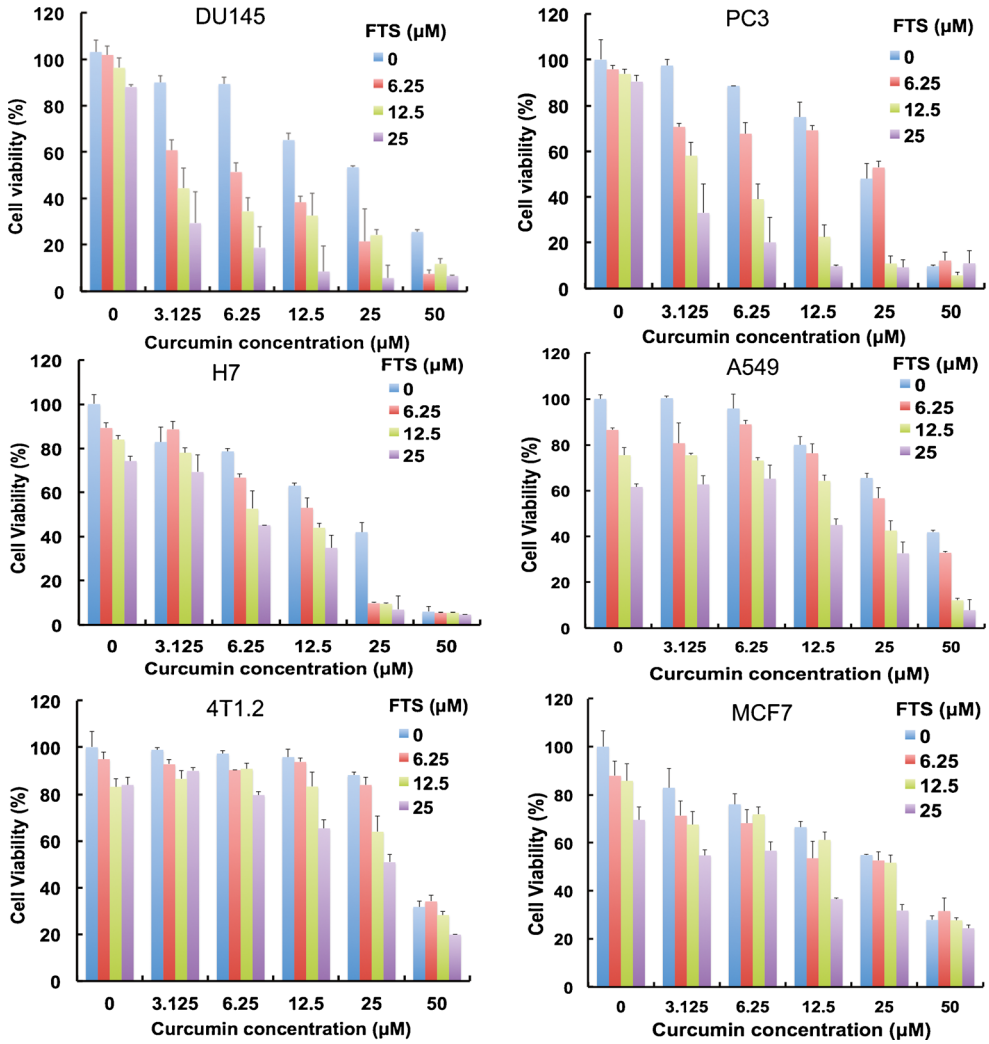

Fig. 1. Synergistic action between FTS and curcumin in inhibiting the proliferation of tumor cells. Various types of tumor cells including DU145, PC3, H7, A549, 4T1.2, and MCF7 cells were treated with various concentrations of free FTS, free curcumin, and combination of both respectively for 96 h, and the cytotoxicity was determined by MTT assay. The experiment was performed in triplicate and repeated three times. Data are presented as means ± standard deviation

Western Blot Analyses

Western blotting was performed to evaluate the protein expression levels of phospho-AKT in DU145 cells. Cells grown in six-wells plates with 80% confluency were treated with free PEG_{5K}-FTS_2(L) or PEG_{5K}-FTS_2(S) micelles, free curcumin, and curcumin-loaded micelles respectively for 12 h. Cells were washed twice with pre-cooled PBS and lysed in a buffer containing 0.2% Triton X-100 for 10 min on ice. Protein concentrations were determined, and equal amounts

Table I. Synergistic Antiproliferative Activity of Curcumin and FTS in Cancer Cells

Drug combination	Cell line	d1 (μM)	$D_{50}1$	d2 (μM)	$D_{50}2$	CI
Curcumin+FTS	DU145	25	68.0±2.0	2.3±0.1	24.3±2.5	0.46
	PC3	25	75.3±4.6	2.5±1.2	29.0±1.3	0.42
	H7	25	70.5±0.7	9.6±0.2	22.5±4.7	0.78
	A549	25	58.0±2.3	20.3±1.4	42.2±3.5	0.91
	4T1.2	25	56.4±0.6	24.5±3.4	46.0±2.1	0.98
	MCF7	25	68.2±4.6	8.3±2.3	28.8±2.0	0.65

Combination Index (CI) of simultaneous treatment of curcumin and farnesylthiosalicylic acid (FTS) in DU145, PC3, H7, A549, 4T1.2, MCF7 cells. Cells were treated with a combination of curcumin and FTS and cell viability was determined by MTT assay. The CI was calculated by the formula: $CI=(d1/D_{50}1)+(d2/D_{50}2)$, where $D_{50}1$ is the concentration of FTS required to produce 50% effect alone, and d1 is the concentration of FTS required to produce the same 50% effect in combination with d2. $D_{50}2$ is similarly the concentration of curcumin required to produce 50% effect alone, and d2 is the concentration of curcumin required to produce the same 50% effect in combination with d1. The CI values are interpreted as follows: <1.0, synergism; 1.0, additive; and >1.0, antagonism. Each experiment was done in triplicate

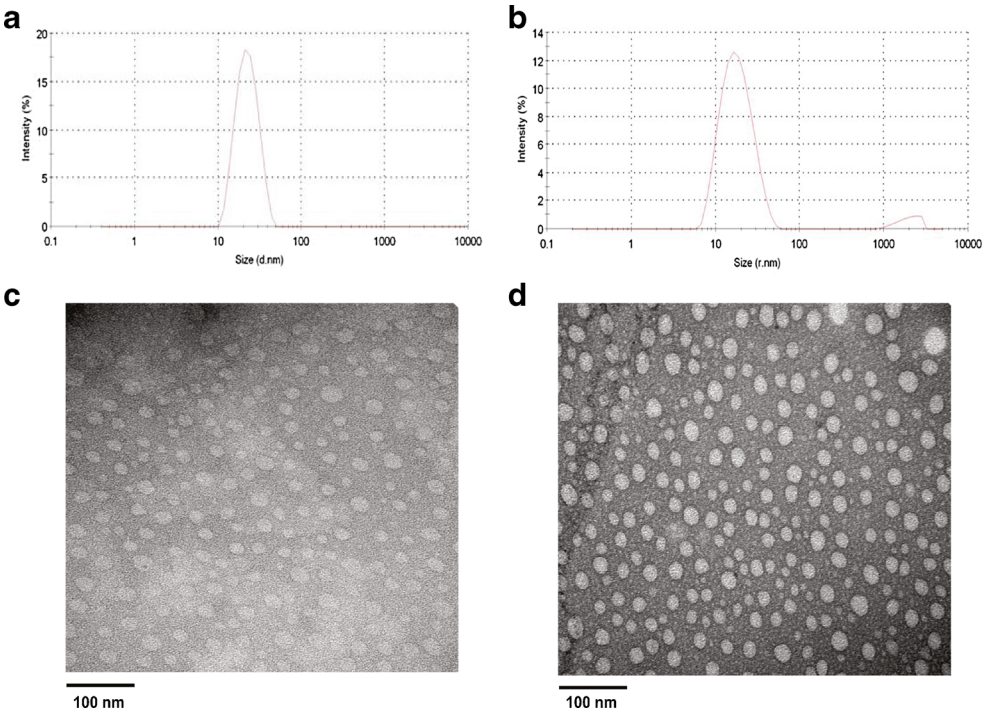

Fig. 2. Particle size distribution and morphology of curcumin/PEG_{5K}-FTS_2 micelles. The average size and size distribution of drug-free micelles (**a**) and curcumin-loaded PEG_{5K}-FTS_2 micelles (**b**) were examined *via* DLS analysis. The morphology of drug-free micelles (**c**) and curcumin-loaded PEG_{5K}-FTS_2 micelles (**d**) was examined *via* EM following negative staining

of total protein lysate were resolved on a 15% SDS-PAGE and subsequently transferred to a nitrocellulose membrane. Membranes were blocked with 5% nonfat milk in PBS for 1 h prior to incubation with rabbit p-Akt or Akt primary antibody dissolved in PBST (DPBS with 0.1% Tween 20) overnight at 4°C. The blots were washed with PBST and then probed with goat antirabbit IgG for 1 h at room temperature followed by chemiluminescence detection. β-Actin was used as a loading control.

Transfection Assay

Transient transfections were performed on DU145 cells using the UF-2 transfection agent as described previously (29). Briefly, the plasmid-UF2 complexes were formed by incubating 0.01 mg of NF-κB reporter gene and 0.04 mg of UF-2 transfection agent at room temperature for 20 min in a total volume of 400 μL of serum-free DMEM medium. The complexes were then mixed with freshly trypsinized cells in 5% FBS cell culture medium, and the cells were added to a 96-well plate at 50–70% confluency. After 12 h of incubation, the transfection medium was replaced with medium that contained 10% fetal bovine serum laced with the designated concentrations of free FTS, free curcumin, free PEG_{5K}-FTS_2(L) or PEG_{5K}-FTS_2(S) micelles, and curcumin-loaded PEG_{5K}-FTS_2(L) or PEG_{5K}-FTS_2(S) micelles respectively. Cells were lysed with 0.2% Triton X-100 12 h later and assayed for luciferase activities. Transfection experiments were performed on at least three occasions, and in each case, experiments were done in triplicate. Data were represented as fold induction over reporter gene alone.

In Vivo Therapeutic Study

The syngeneic mouse tumor model 4T1 was generated by s.c. injection of 2×10^5 cells in 100 μL PBS into the right flank of each female BALB/c mouse. When the tumors reached ~50 mm^3 in size, mice were randomized into four groups (N=5) for treatment. Mice were injected intravenously every other day for six times with 200 μL saline, blank PEG_{5K}-FTS_2(L) micelles, curcumin in Cremophor EL (20 mg/kg), and curcumin-loaded

Table II. Biophysical Characteristics of Curcumin-Loaded PEG_{5K}-FTS_2(L) Micelles and Free Micelles

Micelles	Molar ratio	Particle size (nm)	PDI	DLE (%)	DLC (%)	Stability (h)
PEG_{5K}-FTS_2(L)	–	19.8±0.1	0.266	–	–	–
PEG_{5K}-FTS_2(L): curcumin	0.5:1	24.2±0.6	0.139	75.2	11.8	2
	1:1	20.8±1.0	0.332	89.1	5.9	4
	2.5:1	19.0±1.3	0.239	98.5	2.4	36
	5:1	22.9±1.2	0.080	97.6	1.2	96
	10:1	21.3±0.3	0.145	98.2	0.6	180

Curcumin concentration in micelles was 1 mg/ml. Blank micelles concentration was 20 mg/ml. Values reported at the means±SEM
PDI polydispersity index, *DLE* drug-loading efficiency, *DLC* drug-loading capacity

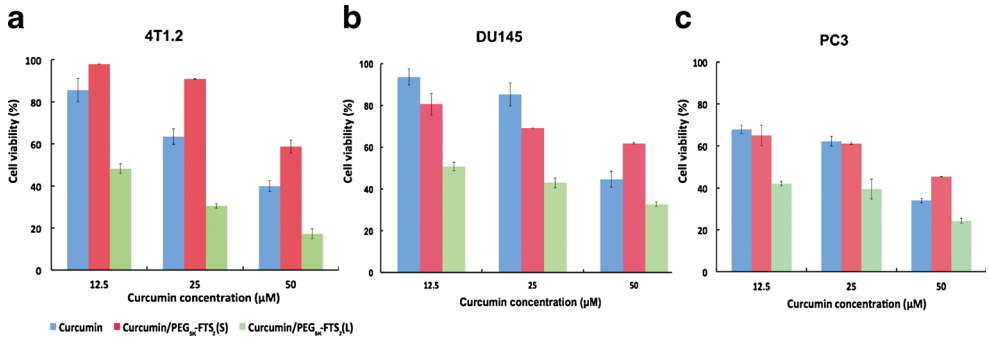

Fig. 3. Cytotoxicity of free curcumin, curcumin/PEG_{5K}-FTS_2 (L), and curcumin/PEG_{5K}-FTS_2 (S) against mouse breast cancer cell line, 4T1.2 (**a**) and human prostate cancer cell lines, DU145 (**b**), and PC3 (**c**). Cells were treated for 96 h and cytotoxicity was determined by MTT assay. Values are reported as the means ± standard deviation for triplicate samples

PEG_{5K}-FTS_2(L) micelles (20 mg/kg) respectively. Tumor sizes and body weights were monitored every 2 days. Tumor volume was calculated according to the formula: volume=(tumor length×tumor width^2)/2. To compare between groups, relative tumor volume (RTV=V/V_0, V_0 was the tumor volume prior to the first injection) was calculated for each measurement. The mice were sacrificed when the tumors became larger than 1.5 cm in diameter or developed ulceration.

Statistical Analysis

In all statistical analyses, the significance was set at a probability of $P<0.05$. All results were reported as the means ±standard deviation. Statistical analysis was performed by Student's *t* test for two groups and one-way ANOVA for multiple groups, followed by Newman–Keuls test if $P<0.05$.

RESULTS

Effect of FTS and Curcumin on Cancer Cell Growth

The growth inhibitory activity of curcumin and FTS was assessed in a broad range of cancer cell lines including DU145 and PC3 (prostate), A549 (lung), H7 (pancreas), and 4T1 and MCF7 (breast). Curcumin or FTS caused a concentration-dependent inhibition of proliferation in all six cell lines (Fig. 1), which was consistent with literature reports (3,20,30–32). When we fixed the concentration of curcumin and gradually increased the concentration of FTS in co-treatment, the inhibition effect was progressively increased with increasing FTS concentration, indicating more effective tumor-killing effect in the combination treatment (Fig. 1). Table I compares the cytotoxicity of single treatment and that of combination treatment at a representative FTS concentration of 25 μM in combination with curcumin. We calculated the combination index (CI) after co-administration of FTS and curcumin to assess whether the combination could confer synergistic, additive, or antagonistic effects (Table I). CI was calculated by the equation CI = (d1/D_{50}1)+(d2/D_{50}2), with D_{50}1 being the concentration of FTS producing 50% cell-killing effect in single treatment and d1 being the FTS concentration required to achieve the same 50% killing effect with d2 in co-treatment. Similarly, D_{50}2 is the concentration of curcumin producing 50% killing effect in single treatment, and d2 is the curcumin concentration required to obtain the same 50% cell-killing effect in combination with d1. A CI of <1, =1, and >1 is suggestive of synergism, additive effect, and antagonism, respectively (33). Data in Table I indicated that the combination of FTS and curcumin showed synergism in all of these examined cancer cell lines.

Characterizations of Curcumin-Loaded PEG_{5K}-FTS_2 Micelles

We have previously shown that a micellar system based on PEG_{5K}-FTS_2(L) retained the biological activity of FTS and was capable of synergistic delivery of paclitaxel (27). Following demonstration of synergy between curcumin and FTS in antitumor activity in various types of tumor cells, we then investigated whether curcumin can be formulated in PEG_{5K}-FTS_2(L) micelles, leading to effective co-delivery of PEG-derivatized FTS and curcumin and the subsequent synergistic action between the two at the tumor site.

Figure 2a shows that the particle size of PEG_{5K}-FTS_2(L) was around 20 nm, which was consistent with our previous report (27). Incorporation of curcumin into PEG_{5K}-FTS_2(L) micelles had minimal impact on the average size and their size distribution (Fig. 2b). TEM shows that both drug-free and curcumin-loaded PEG_{5K}-FTS_2(L) micelles had spherical shape and were homogenous in size distribution (Fig. 2c, d), which was consistent with the result of DLS analysis (Fig. 2a, b).

Table II shows the DLC and DLE at various carrier/drug molar ratios. Curcumin could be formulated in PEG_{5K}-FTS_2(L) micelles at a carrier/drug molar ratio as low as 0.5:1. However,

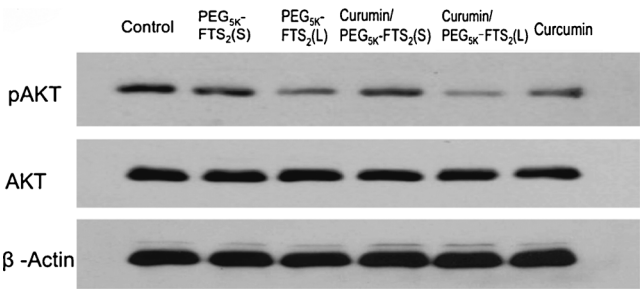

Fig. 4. Inhibitory effect of micellar curcumin on AKT signaling in human prostate cancer cells, DU145. Cells grown in medium containing 2.5% FBS were treated with 0.1% DMSO (control), PEG_{5K}-FTS_2(L), PEG_{5K}-FTS_2(S), curcumin/PEG_{5K}-FTS_2(L), curcumin/PEG_{5K}-FTS_2(S), and free curcumin respectively for 12 h. Western blotting was performed with total protein extracts using antibody against phospho-AKT. The same blot was reprobed with antibodies against total AKT as an internal control and β-Actin as a loading control

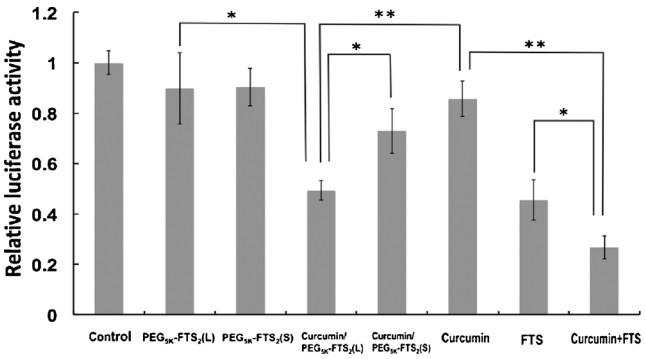

Fig. 5. Inhibitory effect of micellar curcumin on NF-κB activity as determined in a NF-κB reporter assay. DU145 cells were transfected with NF-κB reporter gene. At 12 h post-transfection, cells were treated with free PEG_{5K}-FTS_2, free curcumin, and curcumin-loaded PEG_{5K}-FTS_2 respectively for 12 h. The firefly luciferase activity was normalized and expressed as fold induction over untreated control. Results are presented as means ± standard deviation of the data from three independent experiments performed in triplicate. *P<0.05; **P<0.01

the resulting mixed micelles were only stable for 2 h. Increasing the carrier/drug molar ratio was associated with an improvement in the colloidal stability of the curcumin-loaded micelles. Almost all of the input curcumin was loaded into the PEG_{5K}-FTS_2 micelles at a carrier/drug ratio of 2.5:1, and the resulting mixed micelles were stable for about 36 h. Curcumin/PEG_{5K}-FTS_2 mixed micelles prepared under this condition were used for all subsequent studies.

In Vitro Cytotoxicity of Curcumin/PEG_{5K}-FTS_2 Mixed Micelles

Curcumin was loaded into PEG_{5K}-FTS_2(L) and PEG_{5K}-FTS_2(S) micelles. Figure 3a shows the cytotoxicity of free curcumin and curcumin-formulated micelles in 4T1.2 cells. It was apparent that curcumin formulated in PEG_{5K}-FTS_2(L) micelles was more active than free curcumin in inhibiting the proliferation of tumor cells. Similar results were observed in DU145 (Fig. 3b) and PC3 (Fig. 3c) cancer cells. Interestingly, curcumin formulated in PEG_{5K}-FTS_2(S) micelles was comparable to free curcumin among the three cell lines tested (Fig. 3a–c).

Effect of Curcumin/FTS Combination on AKT and NF-κB Pathways

To investigate the mechanism for the improved inhibitory effect of curcumin/ PEG_{5K}-FTS_2(L) mixed micelles on cancer cells, we examined their effect on AKT and NF-κB pathways in DU145 cells as the two signaling pathways are critically involved in the rapid proliferation of various types of cancer cells (6,7,34,35), and both FTS and curcumin have been shown to negatively regulate the two pathways (6,7,35). As shown in Fig. 4, the level of pAKT was significantly down-regulated following treatment with curcumin, which was consistent with previous reports (5,10,36). The pAKT level was also decreased following treatment with either PEG_{5K}-FTS_2(L) or PEG_{5K}-FTS_2(S), although PEG_{5K}-FTS_2(L) was more effective compared to PEG_{5K}-FTS_2(S). It was also apparent that curcumin formulated in PEG_{5K}-FTS_2(L) micelles was more effective in inhibiting the phosphorylation of AKT compared to the treatment of either alone (Fig. 4).

Figure 5 shows the effect of FTS and curcumin on NF-κB signaling as examined in a NF-κB reporter assay. NF-κB activity was significantly inhibited by treatment with either curcumin or FTS alone. However, the inhibition of NF-κB activity was further enhanced by the combination treatment. It is also apparent that curcumin formulated in PEG_{5K}-FTS_2(L) micelles was more effective in inhibiting NF-κB signaling compared to PEG_{5K}-FTS_2(L) micelles alone or curcumin formulated in PEG_{5K}-FTS_2(S) micelles (Fig. 5).

In Vivo Therapeutic Study

A highly metastatic 4T1.2 model (s.c.) was used to evaluate the *in vivo* antitumor activity of curcumin formulated in PEG_{5K}-FTS_2(L) micelles. Curcumin formulated in Cremophor EL was used as a control. As shown in Fig. 6a, treatment with curcumin/Cremophor EL (six times, every other day) led to a modest inhibition of tumor growth at the early stage. However, there is a rebound in the growth rate of tumor following discontinuation of the treatment after d10. At d20, the tumors in curcumin/Cremophor EL-treated group became comparable to the tumors in PBS group in size.

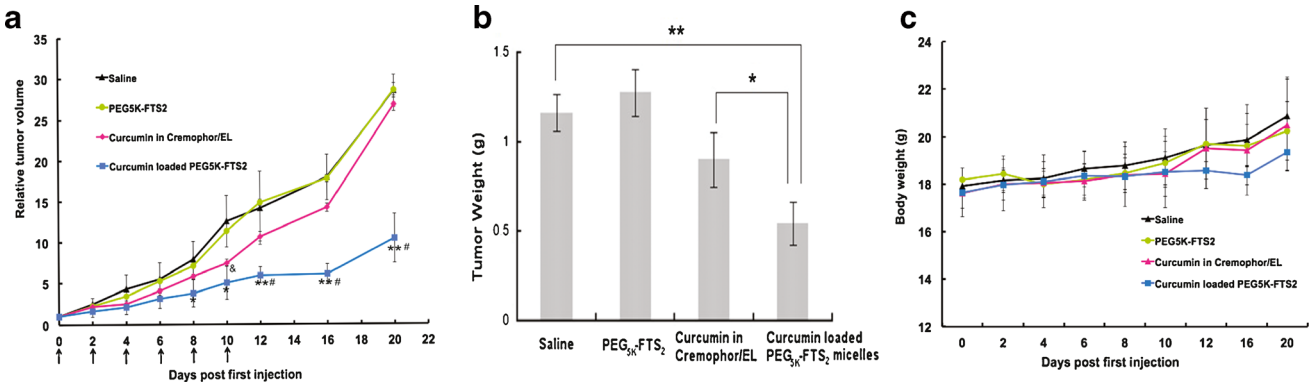

Fig. 6. Enhanced antitumor activity of curcumin formulated in PEG_{5K}-FTS_2 (L) micelles. BALB/c mice were inoculated s.c. with 4T1.2 cells (2×10^5 cells/mouse). Mice with palpable tumors received various treatments every other day and tumor growth and mouse body weight were followed. Tumors were collected at the end of the experiment and weighed. **a** Changes of relative tumor volume at different times following the first treatment. Significant improvement in antitumor activity was found for the curcumin-loaded PEG_{5K}-FTS_2 group compared with the control group (*P<0.05; **P<0.01; N=5) and the group of curcumin formulated in Cremophor/EL ($^{\#}P$<0.05; N=5). Curcumin formulated in Cremophor/EL had moderate tumor inhibitory effect at the early stage when compared to control group (&P<0.05; N=5). **b** Weights of tumors collected at the end of the experiment (*P<0.05; **P< 0.01; N=5). **c** Change of mouse body weight at different times following the first treatment

Curcumin formulated in PEG_{5K}-FTS_2(L) micelles was significantly more effective than curcumin/Cremophor EL in inhibiting the tumor growth. The growth of the tumors remained significantly retarded following the discontinuation of the treatment after d10. Figure 6b shows the weights of the tumors collected at the end of the therapeutic study, which were consistent with the data of tumor growth curves (Fig. 6a). All of the mice showed no signs of abnormal appearance, and no loss of body weight was found in these mice (Fig. 6c).

DISCUSSION

In this study, we have demonstrated for the first time significant synergistic effect between curcumin and FTS in various types of cancers. We have also shown that curcumin can be effectively formulated in PEG-FTS micellar system, leading to enhanced antitumor activity *in vitro* and *in vivo*.

Various systems have been developed for delivery of curcumin including polymeric micelles, liposomes, and hydrogels (37–49). Several polymeric micellar systems have been examined for delivery of curcumin including methoxy poly(-ethylene glycol)-zein, monomethyl poly(ethylene glycol)-poly(ε-caprolactone), methoxy-poly(ethylene glycol)-poly(-lactic acid)-tris-curcumin, methoxypoly(ethylene glycol)-*b*-poly(ε-caprolactone-*co*-*p*-dioxanone), poly(D,L-lac-tide-*co*-glycolide)-*b*-poly(ethylene glycol)-*b*-poly(D,L-lactide-*co*-glycolide), and stearic acid-*g*-chitosan oligosaccharide micelle (41,43,44,46–49). Incorporation of curcumin into polymeric micelles led to enhanced antitumor activity in a number of tumor models including lung, breast, and colon cancers (40–42,48). Curcumin-loaded micelles have also been shown to effectively inhibit tumor angiogenesis (40,41). However, most of the carrier materials in polymeric drug delivery systems do not have biological activity by themselves. PEG_{5K}-FTS_2(L)-based micelles are derived from a promising anticancer agent and have been demonstrated to well retain FTS-mediated antitumor activity (27). FTS-derivatized system shall be particularly suitable for delivery of curcumin as curcumin and FTS demonstrated significant synergy in various types of cancers (Fig. 1, Table I). Indeed, curcumin formulated in PEG_{5K}-FTS_2 (L) micelles was more active than free curcumin in several cancer cells tested including 4T1.2, DU145, and PC3 (Fig. 3). The improved cytotoxicity of curcumin formulated in PEG_{5K}-FTS_2 (L) micelles might be attributed to a synergistic action between the released curcumin and the free FTS that is cleaved from the PEG_{5K}-FTS_2 (L) conjugate following intracellular delivery of the mixed micelles. Another important mechanism might involve the protection of curcumin from decomposition by the PEG_{5K}-FTS_2 (L) micelles. Curcumin is known to undergo rapid degradation in a culture medium or buffer with physiological pH (50,51), and incorporation of curcumin into a delivery system has been shown to improve its bioavailability *via* slowing down the process of decomposition (43,52). Interestingly, curcumin formulated in PEG_{5K}-FTS_2(S)-based micelles was comparable to or slightly less active than free curcumin in inhibiting the growth of cultured tumor cells (Fig. 3). It might be due to the fact that PEG-FTS was largely designed for *in vivo* delivery and that *in vitro* cellular uptake of curcumin delivered *via* PEG-FTS micelles might be less efficient than that of free curcumin due to the steric hindrance imposed by PEG. This was supported by the data that the cytotoxicity of curcumin/PEG_{5K}-FTS_2(L) mixed micelles is less active than the combination of free curcumin and FTS (Figs. 1 and 3). It is possible that the PEG-FTS system can be further improved *via* incorporation of an active targeting ligand to facilitate intracellular delivery of curcumin/PEG-FTS mixed micelles.

The mechanism for the synergy between FTS and curcumin is not clearly understood at present. However, FTS and curcumin are known to inhibit both NF-κB and PI3K/AKT signaling pathways (6,7,32,35,36). Our preliminary data clearly showed a synergy between curcumin and FTS in inhibiting either PI3K/AKT or NF-κB signaling, which likely contributes to the synergistic antitumor effect of the combination treatment.

The *in vivo* antitumor activity of curcumin/PEG_{5K}-FTS_2(L) mixed micelles was examined in a syngeneic mouse tumor model, 4T1.2. 4T1.2 is an aggressive, metastatic breast cancer model. Although treatment with curcumin formulated in Cremophor/EL led to a modest inhibition of tumor growth at the early stage, there was a rapid rebound in the growth rate of the tumor. In contrast, tumor growth was inhibited by curcumin/PEG_{5K}-FTS_2(L) mixed micelles in a more potent, sustained manner. A number of mechanisms are likely to be involved in the improved antitumor activity of curcumin formulated in PEG_{5K}-FTS_2(L) micelles. First, PEG-FTS formed very small-sized mixed micelles with curcumin. Such small sizes (20~30 nm) shall ensure effective penetration into various types of solid tumors including poorly vascularized tumors (53,54). In addition, the potential synergistic antitumor activity between curcumin and the freed FTS will contribute to the overall improved antitumor activity. More studies are currently underway in our laboratory to further improve the PEG-FTS-based delivery system and to better understand the molecular mechanism for the improved antitumor activity of the nanomicellar curcumin.

ACKNOWLEDGMENTS

This work was supported in part by NIH grants R21CA173887, RO1CA174305, and R01GM102989. We would like to thank Dr. Raman Venkataramanan and Mr. Wenchen Zhao for their help in the HPLC analysis of curcumin.

REFERENCES

1. Duvoix A, Blasius R, Delhalle S, Schnekenburger M, Morceau F, Henry E, *et al.* Chemopreventive and therapeutic effects of curcumin. Cancer Lett. 2005;223(2):181–90. doi:10.1016/j.canlet.2004.09.041.
2. Kawamori T, Lubet R, Steele VE, Kelloff GJ, Kaskey RB, Rao CV, *et al.* Chemopreventive effect of curcumin, a naturally occurring anti-inflammatory agent, during the promotion/progression stages of colon cancer. Cancer Res. 1999;59(3):597–601.
3. Aggarwal BB, Shishodia S, Takada Y, Banerjee S, Newman RA, Bueso-Ramos CE, *et al.* Curcumin suppresses the paclitaxel-induced nuclear factor-kappaB pathway in breast cancer cells and inhibits lung metastasis of human breast cancer in nude mice. Clin Cancer Res Off J Am Assoc Cancer Res. 2005;11(20):7490–8. doi:10.1158/1078-0432.CCR-05-1192.
4. Lim GP, Chu T, Yang F, Beech W, Frautschy SA, Cole GM. The curry spice curcumin reduces oxidative damage and amyloid

pathology in an Alzheimer transgenic mouse. J Neurosci Off J Soc Neurosci. 2001;21(21):8370–7.
5. Reuter S, Eifes S, Dicato M, Aggarwal BB, Diederich M. Modulation of anti-apoptotic and survival pathways by curcumin as a strategy to induce apoptosis in cancer cells. Biochem Pharmacol. 2008;76(11):1340–51. doi:10.1016/J.Bcp.2008.07.031.
6. Mukhopadhyay A, Bueso-Ramos C, Chatterjee D, Pantazis P, Aggarwal BB. Curcumin downregulates cell survival mechanisms in human prostate cancer cell lines. Oncogene. 2001;20(52):7597–609. doi:10.1038/Sj.Onc.1204997.
7. Kunnumakkara AB, Anand P, Aggarwal BB. Curcumin inhibits proliferation, invasion, angiogenesis and metastasis of different cancers through interaction with multiple cell signaling proteins. Cancer Lett. 2008;269(2):199–225. doi:10.1016/J.Canlet.2008.03.009.
8. Chen YR, Tan TH. Inhibition of the c-Jun N-terminal kinase (JNK) signaling pathway by curcumin. Oncogene. 1998;17(2):173–8. doi:10.1038/Sj.Onc.1201941.
9. Singh S, Aggarwal BB. Activation of transcription factor NF-kappa B is suppressed by curcumin (diferuloylmethane) [corrected]. J Biol Chem. 1995;270(42):24995–5000.
10. Chaudhary LR, Hruska KA. Inhibition of cell survival signal protein kinase B/Akt by curcumin in human prostate cancer cells. J Cell Biochem. 2003;89(1):1–5. doi:10.1002/jcb.10495.
11. Lev-Ari S, Strier L, Kazanov D, Madar-Shapiro L, Dvory-Sobol H, Pinchuk I, *et al*. Celecoxib and curcumin synergistically inhibit the growth of colorectal cancer cells. Clin Cancer Res Off J Am Assoc Cancer Res. 2005;11(18):6738–44. doi:10.1158/1078-0432.CCR-05-0171.
12. Lev-Ari S, Vexler A, Starr A, Ashkenazy-Voghera M, Greif J, Aderka D, *et al*. Curcumin augments gemcitabine cytotoxic effect on pancreatic adenocarcinoma cell lines. Cancer Investig. 2007;25(6):411–8. doi:10.1080/07357900701359577.
13. Notarbartolo M, Poma P, Perri D, Dusonchet L, Cervello M, D'Alessandro N. Antitumor effects of curcumin, alone or in combination with cisplatin or doxorubicin, on human hepatic cancer cells. Analysis of their possible relationship to changes in NF-kB activation levels and in IAP gene expression. Cancer Lett. 2005;224(1):53–65. doi:10.1016/j.canlet.2004.10.051.
14. Rotblat B, Ehrlich M, Haklai R, Kloog Y. The Ras inhibitor farnesylthiosalicylic acid (Salirasib) disrupts the spatiotemporal localization of active Ras: a potential treatment for cancer. Method Enzymol. 2008;439:467–89. doi:10.1016/S0076-6879(07)00432-6.
15. Marom M, Haklai R, Benbaruch G, Marciano D, Egozi Y, Kloog Y. Selective-inhibition of Ras-dependent cell-growth by farnesylthiosalicylic acid. J Biol Chem. 1995;270(38):22263–70.
16. Kloog Y, Cox AD. RAS inhibitors: potential for cancer therapeutics. Mol Med Today. 2000;6(10):398–402.
17. Blum R, Kloog Y. Tailoring Ras-pathway—inhibitor combinations for cancer therapy. Drug Resist Updat Rev Commentaries Antimicrob Anticancer Chemother. 2005;8(6):369–80. doi:10.1016/j.drup.2005.11.002.
18. McLaughlin SK, Olsen SN, Dake B, De Raedt T, Lim E, Bronson RT, *et al*. The RasGAP gene, RASAL2, is a tumor and metastasis suppressor. Cancer Cell. 2013;24(3):365–78. doi:10.1016/j.ccr.2013.08.004.
19. Min J, Zaslavsky A, Fedele G, McLaughlin SK, Reczek EE, De Raedt T, *et al*. An oncogene-tumor suppressor cascade drives metastatic prostate cancer by coordinately activating Ras and nuclear factor-kappaB. Nat Med. 2010;16(3):286–94. doi:10.1038/nm.2100.
20. Gana-Weisz M, Halaschek-Wiener J, Jansen B, Elad G, Haklai R, Kloog Y. The Ras inhibitor S-trans, trans-farnesylthiosalicylic acid chemosensitizes human tumor cells without causing resistance. Clin Cancer Res. 2002;8(2):555–65.
21. Kloog Y, Cox AD, Sinensky M. Concepts in Ras-directed therapy. Expert Opin Investig Drugs. 1999;8(12):2121–40. doi:10.1517/13543784.8.12.2121.
22. Haklai R, Elad-Sfadia G, Egozi Y, Kloog Y. Orally administered FTS (salirasib) inhibits human pancreatic tumor growth in nude mice. Cancer Chemother Pharmacol. 2008;61(1):89–96. doi:10.1007/s00280-007-0451-6.
23. Biran A, Brownstein M, Haklai R, Kloog Y. Downregulation of survivin and aurora A by histone deacetylase and RAS inhibitors: a new drug combination for cancer therapy. Int J Cancer J Int Cancer. 2011;128(3):691–701. doi:10.1002/ijc.25367.
24. Mologni L, Brussolo S, Ceccon M, Gambacorti-Passerini C. Synergistic effects of combined Wnt/KRAS inhibition in colorectal cancer cells. PLoS ONE. 2012;7(12):e51449. doi:10.1371/journal.pone.0051449.
25. Anand P, Kunnumakkara AB, Newman RA, Aggarwal BB. Bioavailability of curcumin: problems and promises. Mol Pharm. 2007;4(6):807–18. doi:10.1021/mp700113r.
26. Kraitzer A, Kloog Y, Haklai R, Zilberman M. Composite fiber structures with antiproliferative agents exhibit advantageous drug delivery and cell growth inhibition in vitro. J Pharm Sci. 2011;100(1):133–49. doi:10.1002/jps.22238.
27. Zhang XL, Lu JQ, Huang YX, Zhao WC, Chen YC, Li J, *et al*. PEG-farnesylthiosalicylate conjugate as a nanomicellar carrier for delivery of paclitaxel. Bioconjug Chem. 2013;24(3):464–72. doi:10.1021/Bc300608h.
28. Huang YX, Lu JQ, Gao X, Li J, Zhao WC, Sun M, *et al*. PEG-derivatized embelin as a dual functional carrier for the delivery of paclitaxel. Bioconjug Chem. 2012;23(7):1443–51. doi:10.1021/Bc3000468.
29. Gao X, Huang L. Potentiation of cationic liposome-mediated gene delivery by polycations. Biochemistry. 1996;35(3):1027–36. doi:10.1021/bi952436a.
30. Ramachandran C, Fonseca HB, Jhabvala P, Escalon EA, Melnick SJ. Curcumin inhibits telomerase activity through human telomerase reverse transcriptase in MCF-7 breast cancer cell line. Cancer Lett. 2002;184(1):1–6.
31. McPherson RA, Conaway MC, Gregory CW, Yue W, Santen RJ. The novel ras antagonist, farnesylthiosalicylate, suppresses growth of prostate cancer in vitro. Prostate. 2004;58(4):325–34. doi:10.1002/Pros.10336.
32. Starkel P, Charette N, Borbath I, Schneider-Merck T, De Saeger C, Abarca J, *et al*. Ras inhibition in hepatocarcinoma by S-trans-trans-farnesylthiosalicylic acid: association of its tumor preventive effect with cell proliferation, cell cycle events, and angiogenesis. Mol Carcinog. 2012;51(10):816–25. doi:10.1002/mc.20849.
33. Steel GG, Peckham MJ. Exploitable mechanisms in combined radiotherapy-chemotherapy: the concept of additivity. Int J Radiat Oncol Biol Phys. 1979;5(1):85–91.
34. Kinkade CW, Castillo-Martin M, Puzio-Kuter A, Yan J, Foster TH, Gao H, *et al*. Targeting AKT/mTOR and ERK MAPK signaling inhibits hormone-refractory prostate cancer in a preclinical mouse model. J Clin Invest. 2008;118(9):3051–64. doi:10.1172/Jci34764.
35. Smalley KS, Eisen TG. Farnesyl thiosalicylic acid inhibits the growth of melanoma cells through a combination of cytostatic and pro-apoptotic effects. Int J Cancer J Int Cancer. 2002;98(4):514–22.
36. Aoki H, Takada Y, Kondo S, Sawaya R, Aggarwal BB, Kondo Y. Evidence that curcumin suppresses the growth of malignant gliomas in vitro and in vivo through induction of autophagy: role of Akt and extracellular signal-regulated kinase signaling pathways. Mol Pharmacol. 2007;72(1):29–39. doi:10.1124/mol.106.033167.
37. Li L, Braiteh FS, Kurzrock R. Liposome-encapsulated curcumin: in vitro and in vivo effects on proliferation, apoptosis, signaling, and angiogenesis. Cancer. 2005;104(6):1322–31. doi:10.1002/cncr.21300.
38. Yallapu MM, Jaggi M, Chauhan SC. Curcumin nanoformulations: a future nanomedicine for cancer. Drug Discov Today. 2012;17(1–2):71–80. doi:10.1016/j.drudis.2011.09.009.
39. Lin YL, Liu YK, Tsai NM, Hsieh JH, Chen CH, Lin CM, *et al*. A Lipo-PEG-PEI complex for encapsulating curcumin that enhances its antitumor effects on curcumin-sensitive and curcumin-resistance cells. Nanomed Nanotechnol. 2012;8(3):318–27. doi:10.1016/J.Nano.2011.06.011.
40. Liu L, Sun L, Wu QJ, Guo WH, Li L, Chen YS, *et al*. Curcumin loaded polymeric micelles inhibit breast tumor growth and spontaneous pulmonary metastasis. Int J Pharm. 2013;443(1–2):175–82. doi:10.1016/J.Ijpharm.2012.12.032.
41. Gong CY, Deng SY, Wu QJ, Xiang ML, Wei XW, Li L, *et al*. Improving antiangiogenesis and anti-tumor activity of curcumin by

biodegradable polymeric micelles. Biomaterials. 2013;34(4):1413–32. doi:10.1016/J.Biomaterials.2012.10.068.
42. Gou M, Men K, Shi H, Xiang M, Zhang J, Song J, *et al*. Curcumin-loaded biodegradable polymeric micelles for colon cancer therapy in vitro and in vivo. Nanoscale. 2011;3(4):1558–67. doi:10.1039/c0nr00758g.
43. Ma Z, Haddadi A, Molavi O, Lavasanifar A, Lai R, Samuel J. Micelles of poly(ethylene oxide)-b-poly(epsilon-caprolactone) as vehicles for the solubilization, stabilization, and controlled delivery of curcumin. J Biomed Mater Res A. 2008;86(2):300–10. doi:10.1002/jbm.a.31584.
44. Podaralla S, Averineni R, Alqahtani M, Perumal O. Synthesis of novel biodegradable methoxy poly(ethylene glycol)-zein micelles for effective delivery of curcumin. Mol Pharm. 2012;9(9):2778–86. doi:10.1021/mp2006455.
45. Sahu A, Kasoju N, Bora U. Fluorescence study of the curcumin-casein micelle complexation and its application as a drug nanocarrier to cancer cells. Biomacromolecules. 2008;9(10):2905–12. doi:10.1021/bm800683f.
46. Yang R, Zhang S, Kong D, Gao X, Zhao Y, Wang Z. Biodegradable polymer-curcumin conjugate micelles enhance the loading and delivery of low-potency curcumin. Pharm Res. 2012;29(12):3512–25. doi:10.1007/s11095-012-0848-8.
47. Song Z, Feng R, Sun M, Guo C, Gao Y, Li L, *et al*. Curcumin-loaded PLGA-PEG-PLGA triblock copolymeric micelles: preparation, pharmacokinetics and distribution in vivo. J Colloid Interface Sci. 2011;354(1):116–23. doi:10.1016/j.jcis.2010.10.024.
48. Wang K, Zhang T, Liu L, Wang X, Wu P, Chen Z, *et al*. Novel micelle formulation of curcumin for enhancing antitumor activity and inhibiting colorectal cancer stem cells. Int J Nanomedicine. 2012;7:4487–97. doi:10.2147/IJN.S34702.
49. Song L, Shen YY, Hou JW, Lei L, Guo SR, Qian CY. Polymeric micelles for parenteral delivery of curcumin: preparation, characterization and in vitro evaluation. Colloid Surf A. 2011;390(1–3):25–32. doi:10.1016/J.Colsurfa.2011.08.031.
50. Wang YJ, Pan MH, Cheng AL, Lin LI, Ho YS, Hsieh CY, *et al*. Stability of curcumin in buffer solutions and characterization of its degradation products. J Pharm Biomed Anal. 1997; 15(12):1867–76.
51. Pan MH, Huang TM, Lin JK. Biotransformation of curcumin through reduction and glucuronidation in mice. Drug Metab Dispos Biol Fate Chem. 1999;27(4):486–94.
52. Mohanty C, Sahoo SK. The in vitro stability and in vivo pharmacokinetics of curcumin prepared as an aqueous nanoparticulate formulation. Biomaterials. 2010;31(25):6597–611. doi:10.1016/j.biomaterials.2010.04.062.
53. Maeda H, Wu J, Sawa T, Matsumura Y, Hori K. Tumor vascular permeability and the EPR effect in macromolecular therapeutics: a review. J Control Release. 2000;65(1–2):271–84. doi:10.1016/S0168-3659(99)00248-5.
54. Cabral H, Matsumoto Y, Mizuno K, Chen Q, Murakami M, Kimura M, *et al*. Accumulation of sub-100 nm polymeric micelles in poorly permeable tumours depends on size. Nat Nanotechnol. 2011;6(12):815–23. doi:10.1038/Nnano.2011.166.